JOURNAL OF MATERIALS SCIENCE **38** (2003) 3611–3617

Effects of alloying elements on microstructural evolution and mechanical properties of induction quenched-and-tempered steels

WON JONG NAM, DAE SUNG KIM
Kookmin University, Seoul 136-702, Korea
E-mail: wjnam@kookmin.ac.kr

SOON TAE AHN
Samhwa R&D Center, Pusan 608-130, Korea

The effects of Cr and/or Mo additions and tempering temperatures on mechanical properties in relation to the microstructural evolution during tempering were investigated in induction-tempered steels. The additions of Cr and/or Mo result in the finer distribution of cementite particles due to the decrease in the coarsening rates of cementite particles above tempering temperature of 400°C, while their influence is less effective at low tempering temperatures. Accordingly, the increments of tensile strength and yield strength by the addition of alloying elements become more pronounced at high temperatures above 400°C. The occurrence of maximum peak of yield strength at 400°C would be related to further precipitation of the cementite at low temperatures, and the subsequent spheroidization and coarsening process of the cementite at high temperatures. The addition of alloying elements does not change the minima in Charpy impact values, related to tempered martensite embrittlement, since alloying elements do not have an influence on the decomposition of retained austenite and the formation of the cementite at boundaries. The strain-hardening exponent, *n*, decreases up to 400°C and then continuously increases with tempering temperature. This abrupt increase of *n* at 300°C is related to the transformation of retained austenite during straining in induction-tempered steels.

1. Introduction

Induction heat treatment has been applied widely in the automotive industry. Besides surface hardening [1], which hardens only the surface layer and gives the surface a high compressive residual stress to improve fatigue characteristics, induction quenching-and-tempering (IQT) process, as a through-hardening method of steels, is known to provide the good combination of high strength and toughness and the less deviation of mechanical properties to steels. The advantages of IQT process include the accurate control of temperature, the short processing time, the less decarburization and the convenience in obtaining refined microstructure.

Recently, hot coiling in the production of automotive suspension springs has been replaced by cold coiling through the application of IQT process [2–5]. Kawasaki *et al*. [5] found that refined austenite grain size and the distribution of fine cementite particles at boundaries could be obtained by the adoption of IQT process due to the rapid heating and short heating time. According to their results, tempered martensite, produced by IQT process, would be expected as a suitable microstructure for the development of high strength spring steel. However, their results were limited to the steels containing high Si content above 1.2 wt%. Generally, Si is known to be effective in refining tempered carbides by delaying the conversion of ε-carbide to cementite during tempering [6–12], although its deleterious effect on surface decarburization and toughness. Thus, the combination effect of the rapid heating in IQT process and high Si content in steels could provide high strength Si-Cr spring steels with excellent mechanical properties through the formation of refined microstructure.

Meanwhile, the elimination of intermediate annealing during cold forging process can provide the significant advantages of cost- and time-saving in manufacturing automotive components. However, for the steels with high strength above 1000 MPa, it is difficult to obtain the good ductility and toughness enough to prevent fracture during high speed deformation of cold forging. Furthermore, the low straining hardening exponent would be required in steels to reduce the variation of hardness in automotive components after cold forging. Tempered martensite with finely distributed spheroidal cementite produced by IQT process, would be expected as one of optimum microstructures, which can satisfy those requirements and be applied directly to

cold forging process of automotive components without intermediate thermal treatment. In addition to IQT process, alloying elements also have a significant effect on microstructures and mechanical properties in steels. The behavior of carbide particles in low alloy steels would react more sensitively to tempering conditions than spring steels containing high Si content. Although the additions of alloying elements such as Cr and Mo, do not affect the behavior of tempered carbides at low tempering temperatures as Si in spring steels, the rates of the spheroidization and the coarsening of the cementite are reduced at a high temperature above 400°C, due to their slow diffusivity [13, 14]. Consequently, the finer interparticle spacing of the cementite can be easily obtained by the additions of alloying elements. Furthermore, the advantage of IQT process would enhance the good combination of high strength and toughness even in steels containing less amount of alloying elements. However, detailed information about the effects of alloying elements and tempering temperatures on microstructures and mechanical properties of IQT processed steels, has yet to be clarified.

In view of the foregoing, the purposes of this investigation are to analyze the effects of Cr and Mo additions and tempering temperatures on the microstructural evolution during induction quenching-and-tempering process, and to examine mechanical properties of IQT processed steels.

2. Experimental procedure

The steels used in this study were hot-rolled with the chemical compositions given in Table I. To investigate the effects of alloying elements, the additions of Cr and Mo were controlled to 1.0% and 0.2%, respectively. Hot-rolled steels with 16 mm in a diameter were induction-heated for 50 seconds, and quenched to room temperature by jet spraying water. The heating temperature of steel A should be kept above 1150°C to obtain the fully austenite structure, while steels B and C containing alloying elements were heated at the low temperature of 950°C to get the smaller austenite grain size. The measured AGS were ASTM No. 7.0 for steel A, 11.0 for steel B and 10.5 for steel C. Then, quenched rods were tempered at temperatures of 300°C–700°C by induction heating for 40 seconds. Additionally, to compare the properties of induction-tempered steels with those by salt bath heating, quenched specimens of steel C were also tempered at temperatures of 300°C–700°C in a molten salt bath for 30 min (steel C-salt).

For a detailed understanding of the microstructural evolution during the heat-treatment, a transmission electron microscope (TEM) was used to analyze thin foils obtained from the samples tempered at various temperatures. TEM samples were prepared by utilizing a conventional jet polishing technique in a mixture of 10% perchloric acid and glacial acetic acid. For tensile tests, rods tempered at various temperatures were machined in the ASTM subsize form of 6.25 mm gauge diameter and 25 mm gauge length. Uniaxial tensile tests were conducted operating at a constant crosshead speed of 1 mm/min. Charpy V-notch specimens were machined from tempered rods, in the ASTM standard form of 10 × 10 × 55 mm. Tensile data and Charpy impact data reported in this study are the average values of the data obtained from five samples and ten samples, respectively, at an each experimental condition.

TABLE I Chemical compositions of steels used in this study

	(wt.%)							
Grade	C	Si	Mn	P	S	Cr	Mo	Aus. temp.
Steel A	0.21	0.27	0.87	0.015	0.004	–	–	1150°C
Steel B	0.19	0.20	0.66	0.014	0.002	0.98	–	950°C
Steel C	0.21	0.22	0.73	0.014	0.012	1.08	0.19	950°C

3. Results and discussion

3.1. Microstructure

Fig. 1 shows transmission electron micrographs of tempered steels at various tempering temperatures. For steel A, a number of rod-like cementite particles, nucleated during the third stage of tempering, are the main microstructural feature observed within martensite laths when tempered at 300°C (Fig. 1a). As tempering temperature increases up to 500°C (Fig. 1b), rod-like cementite particles dissolve and begin to change their shape from the rod type to the spheroidal type, with reducing the aspect ratio of the cementite through a gradual spheroidization. In addition, the cementite film, formed at prior austenite boundaries as well as at the lath boundaries of the martensite during the second stage, would gradually become spheroidized and coarsen into stringer-type cementite particles. At a high tempering temperature of 600°C, the observed microstructure consists of mainly spheroidal cementite and a small amount of rod-like cementie. The further increase of tempering temperature (Fig. 1d) results in the coarsening of cementite particles by an Ostwald ripening type of process. Fig. 1d provides the evidence of spheroidal cementite particles distributed randomly within martensite laths and along boundaries, when tempered at 700°C.

For steel B containing 1.0% Cr (Fig. 1e–h), the relationship between the behavior of tempered carbides and tempering temperature is somewhat different from the trend shown in steel A, considering the tempering temperature which the microstructural evolution occurs. The considerable amount of cementite particles can maintain the rod-like shape up to tempering temperature of 500°C, while some particles within martensite laths start to dissolve (Fig. 1b). The alloying element, Cr, is known to have little effect on the formation and the early growth of the cementite during tempering [13–15]. However, the coarsening behavior of cementite particles at a high tempering temperature is significantly influenced by the diffusion of carbon and alloying element [14–16]. Accordingly, the distribution of cementite particles in Fig. 1g, tempered at 600°C, looks similar to that of steel A, tempered at 500°C, since a low diffusivity of substitutional element would decrease the rates of the spheroidization and coarsening of the cementite. Spheroidal particles within martensite laths and stringers of particles along boundaries in

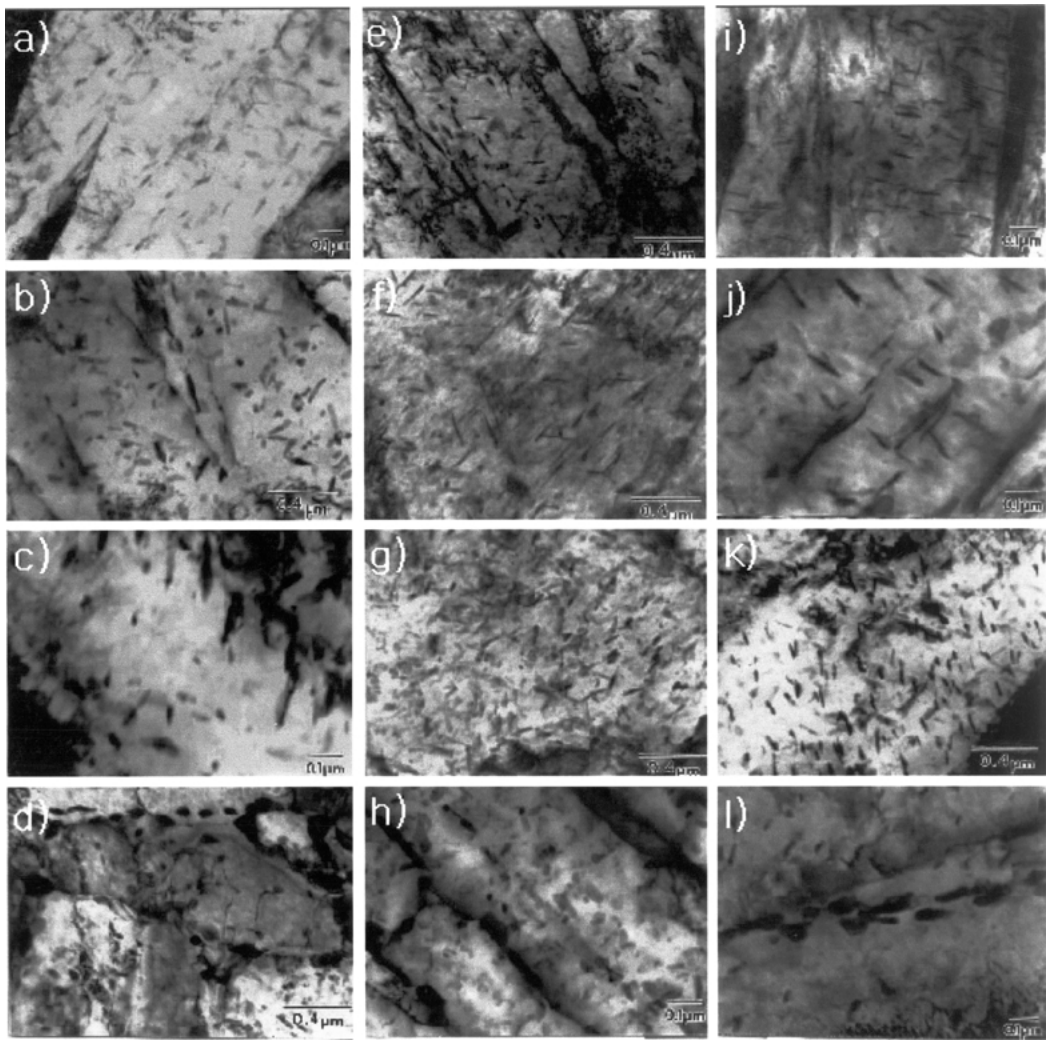

Figure 1 TEM micrographs showing the behavior of tempered carbides during tempering: (a) steel A, 300°C, (b) steel A, 500°C, (c) steel A, 600°C, (d) steel A, 700°C, (e) steel B, 300°C, (f) steel B, 500°C, (g) steel B, 600°C, (h) steel B, 700°C, (i) steel C, 300°C, (j) steel C, 500°C, (k) steel C, 600°C, and (l) steel C, 700°C.

Fig. 1h, show that the coarsening of cementite particles is operative at the tempering temperature of 700°C.

The behavior of tempered carbides with tempering temperature in steel C also shows the similar trends to other steels in the present study, except for the further delay of the spheroidization and coarsening of cementite particles to a higher temperature. The presence of rod-like cementite particles in steel C tempered at 600°C in Fig. 1k, indicates that the alloying elements of Cr and Mo are effective to retard the spheroidization and coarsening of the cementite during tempering.

3.2. Mechanical properties

Microstructural changes discussed above are closely related to the variations of mechanical properties of tempered steels. The variation of tensile strength (TS) with tempering temperature in Fig. 2a shows a general trend that TS continuously decreases as tempering temperature increases. The solid solution hardening effect of alloying elements induces a slight TS increment at the same tempering temperature. However, TS increment with the addition of alloying elements becomes more pronounced at high tempering temperatures above 400°C. Although for steel A the high tensile strength of 1420 MPa tempered at 300°C drops to 830 MPa when tempered at 700°C, steel C shows 530 MPa drop in TS when tempering temperature increases from 300°C to 700°C. This implies that beside the solid solution hardening effect, the addition of alloying elements would affect the progress of matrix softening such as recovery. Additionally, this result would be closely related to the influence of alloying elements, Cr and Mo, on the distribution of tempered carbides at each tempering temperature. At low tempering temperatures, the addition of alloying elements does not significantly affect the behavior of tempered carbides. However, at a high temperature above 400°C, the additions of alloying elements reduce the spheroidization and coarsening rate of the cementite, resulting in the finer particle distribution of the cementite, since Cr and Mo dissolve in the cementite and therefore stabilize the cementite [16, 17]. Accordingly, the additions of alloying elements, Cr and Mo, result in the retardation of the softening at higher tempering temperatures. Meanwhile, the secondary hardening effect due to the precipitation of alloy carbides was not observed below the tempering temperature of 700°C in the present work.

The short tempering time of induction-tempered steels causes the less decrease of TS with tempering

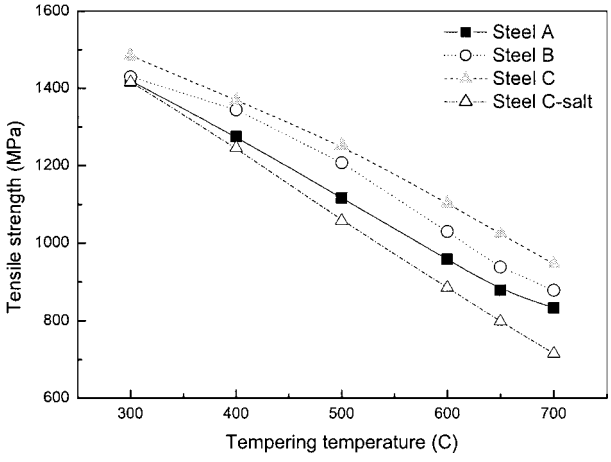

(a)

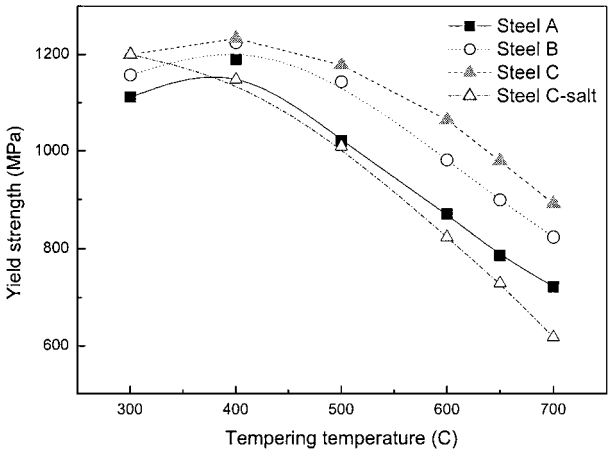

(b)

Figure 2 The variations of (a) tensile strength and (b) yield strength of steels with tempering temperature.

temperature, compared with tempered steels by salt bath heating. The difference of TS between steel C and steel C-salt becomes more pronounced at high tempering temperatures above 500°C. Although the difference of TS between steel C and steel C-salt is only 70 MPa at 300°C tempering, it reaches 250 MPa when tempered at 700°C. The insufficient tempering time for the matrix softening including dislocation annihilation and recovery, results in the retardation of the softening rate at higher tempering temperatures for induction tempered steels.

Fig. 2b shows the plot of yield strength (YS) as a function of tempering temperature for all the tested steels. It first increases with tempering temperature up to 400°C and then continuously decreases with increasing tempering temperature. Since YS is largely affected by the distribution of tempered carbides [17], the occurrence of maximum peak of YS at 400°C would be strongly related to the characteristics of carbides existing at each tempering temperature. At low temperatures of tempering (the early stage of cementite precipitation), the characteristics of cementite particles, i.e., interparticle spacing, volume and shape, etc., would be improper for those particles to effectively hinder the movement of mobile dislocations during straining. Consequently, YS becomes small at a low tempering temperature. However, during subsequent tempering at a high temperature of 400°C, interparticle spacing would decrease due to further precipitation of the cementite. The decrease in YS above tempering temperature of 400°C would be caused by the spheroidization and the coarsening of the cementite, and matrix softening at high tempering temperatures. Meanwhile, the difference of YS among steels tempered at low tempering temperatures can be attributed to the contribution of solid solution hardening in tempered steels.

It is also shown that YS of steel C-salt is lower than that of induction-tempered steel C at tempering temperatures above 400°C. As mentioned before, the longer tempering time in salt bath would result in the lower YS for steel C-salt. Besides, the difference of YS between steels C and C-salt becomes more pronounced at high tempering temperature. YS of steel C-salt tempered at 700°C is lower than that of steel C by 250 MPa. This implies that the softening, due to the spheroidization and coarsening of cementite particles, proceeds more rapidly at high temperature in tempered steels by salt bath heating.

Fig. 3 shows the effect of tempering temperature on ductility. Since the variation of mechanical properties is closely related to the microstructural evolution of the matrix during tempering, the matrix softening and the coarsening of carbide particles can be considered as main factors controlling ductility, such as reduction of area (RA). RA is a measure of the deformation required to produce fracture and is dependent on specimen geometry and deformation behavior. Considering the increase of RA with tempering temperature in Fig. 3, it is obvious that the addition of alloying elements has an influence on the progress of matrix softening as well as the behavior of carbide particles during tempering in the present steel. Generally, the addition of alloying elements decreases ductility in tempered steels, due to the solid solution hardening and the refinement of carbide particles. Accordingly, steel B, containing Cr, shows higher RA than steel C, with Cr and Mo, over all the tempering temperatures. It is interesting to note that RA of the carbon steel (steel A) tempered at 300°C and 400°C is lower than that of alloy steels (steels B and C). At the low tempering temperature below

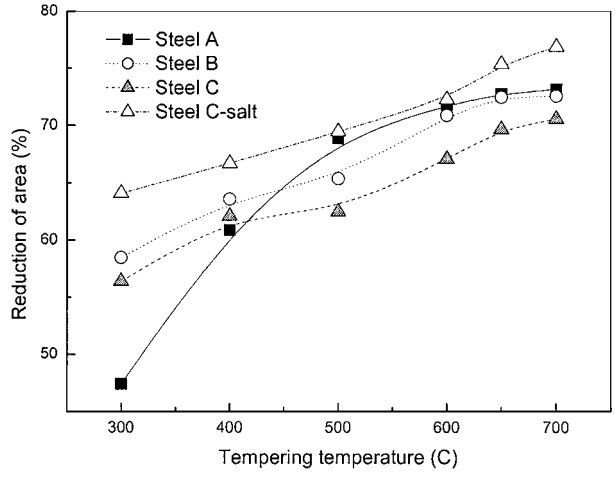

Figure 3 The variations of reduction of area (RA) of steels with tempering temperature.

400°C, tempered steels with high tensile strength above 1200 MPa would behave in a brittle manner during tensile testing, due to the insufficient softening effect of matrix at low tempering temperatures. Thus, ductility, RA, could be significantly affected by the microstructural unit size such as martensite packet or block, which is a function of prior austenite grain size, since boundaries can act as obstacles to crack propagation [18, 19]. Accordingly, the increase of the microstructural unit size, due to the increase of the prior austenite grain size, would result in the lower RA of steel A tempered at 300°C and 400°C than alloy steels. However, at higher tempering temperatures above 400°C, steel A with the larger AGS does not show the less RA than that of steels B and C. This implies that the degree of matrix softening and the distribution of carbide particles become main factors controlling ductility rather than the prior austenite grain size at high tempering temperatures.

The results of Charpy impact test, performed at a room temperature to evaluate toughness of the steels, are presented in Fig. 4. Charpy impact energy responds to tempering temperature in the similar manner to RA in Fig. 3, except for a difference in the shape of curves. The refined AGS in steels B and C tempered below 400°C induces the increment of impact energy over steel A in Fig. 4, since boundaries of martensite packet or block, significantly controlled by the prior austenite grain size, can act as obstacles to crack propagation. It is interesting to note that the minima in the Charpy impact energy curves occur at the intermediate tempering temperature of 400°C for all tempered steels. This attendant loss of impact toughness is known as tempered martensite embrittlement (TME). The observed minimal impact energy values, corresponding to TME, are close to 44J, 82J, and 59J at tempering temperatures of 400°C for steel A, steel B and steel C, respectively. This TME behavior is closely related to the changes in interlath microstructures. According to Speich and Leslie [20], as tempering temperature increases, retained austenite decomposes into the film-type cementite during the second stage of tempering at lath or martensite grain boundaries. In addition, cementite film would grow into thick cementite film or coarsen into stringer-type cementite particles. Thus, it is anticipated that the coarsening or the lateral thickening of the cementite at lath boundaries would be responsible for the occurence of TME, as Peters *et al.* [21] and authors [22] observed in Fe-Cr-Ni-C steels and Si-Cr spring steels, respectively. As mentioned above, the increase of Charpy impact energy above 400°C is associated with the matrix softening and coarsening of cementite particles. Another finding in Fig. 4 is that the minima in Charpy impact energy curves for the present steels are not changed with the content of alloying elements in steels. This fact is evident since alloying elements of Cr and Mo do not have an influence on the decomposition of retained austenite and the formation of the cementite at boundaries [13, 14].

Meanwhile, it is interesting to note that the difference of Charpy impact energy between steels C and C-salt increases abruptly at tempering temperatures above 600°C. This implies that the significant microstructural change occurs when tempering temperature goes above 600°C in steel C-salt. Generally, the microstructural evolution during tempering includes the decomposition of retained austenite, the precipitation and coarsening of cementite particles, accompanying the softening process of matrix as recovery, recrystallization and grain growth. The presence of equiaxed grains with high angle boundaries in steel C-salt (Fig. 5, tempered at temperatures above 600°C), is directly related with the abnormal increase of Charpy impact energy in Fig. 4. Thus, it is thought that of the abnormal

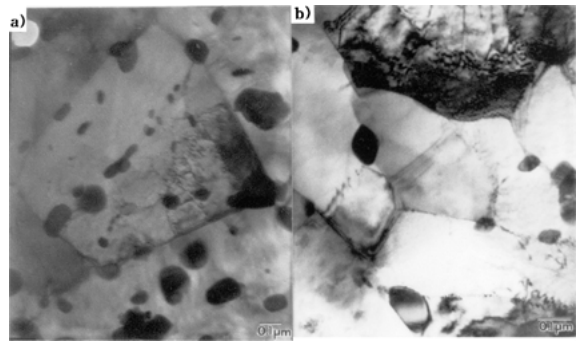

Figure 5 TEM micrographs of the steel C-salt tempered at (a) 650°C and (b) 700°C, showing the presence of recrystallized grains.

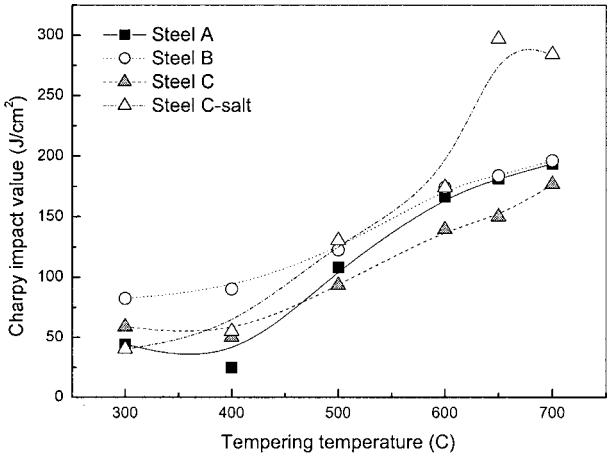

Figure 4 The variations of Charpy impact energy as a function of tempering temperature.

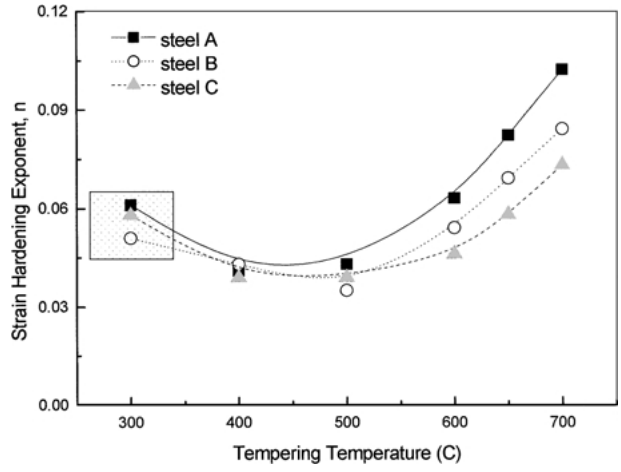

Figure 6 The variations of strain-hardening exponent as a function of tempering temperature.

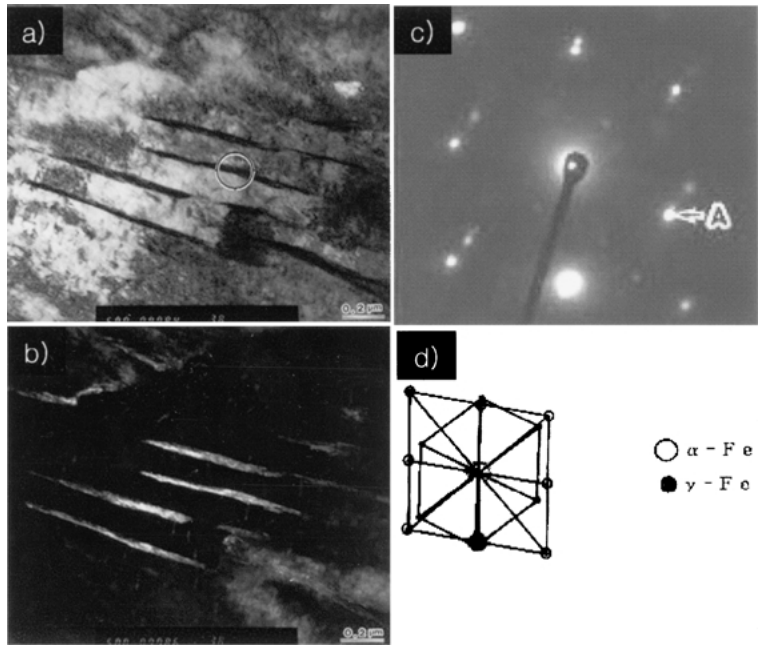

Figure 7 TEM micrographs of retained austenite in steel C tempered at 300°C: (a) bright field image, (b) dark field image, (c) diffraction pattern showing K-S relation, and (d) schematic interpretation of diffraction pattern, showing K-S relation.

increase in Charpy impact energy in steel C-salt would be associated with the process of softening, especially the occurrence of the recrystallization.

The relationship between true stress and true strain in the region of uniform plastic deformation during tensile test can be described by the Ludwik-Holloman equation of the form

$$\sigma = K \cdot \varepsilon^n$$

where σ is the true stress, ε is the true strain, K and n are independent of strain and called the strength coefficient and the strain-hardening exponent, respectively. In a tensile test, true uniform strain is equal to the strain-hardening exponent, that is, $\varepsilon = n$. This strain hardening exponent, n, is a useful parameter to estimate the uniform elongation, the workability and work-hardening rate during the deformation of materials. Gensamer [23] has provided the data for steels with different microstructures to show that the magnitude of n is inversely related to the strength of the steels. Fig. 6 shows the general trend that the magnitude of n increases with tempering temperature, except for the tempering temperature of 300°C. This abrupt increase of n at low tempering temperatures would be attributed to the presence of the retained austenite in steels tempered at 300°C. The retained austenite in Fig. 7 would transform into martensite during straining. Thus, the transformation of retained austenite in steels tempered at 300°C would cause the occurrence of high strain-hardening exponent. Additionally, steel A shows the higher n values than alloy steels as expected.

4. Conclusions

From this investigation about the effects of Cr and/or Mo additions and tempering temperatures on the microstructural evolution and mechanical properties during induction quenching-and-tempering process, the following specific conclusions can be made.

1. Although the additions of alloying elements do not significantly affect the behavior of tempered carbides at low tempering temperatures, they are effective on the retardation of the spheroidization and coarsening of the cementite at high temperatures. Consequently, the transition temperature of the shape in cementite particles from the rod type to the spheroidal type, would be delayed to higher tempering temperatures by the additions of alloying elements.
2. The increment of tensile strength by the addition of alloying elements becomes more pronounced at high tempering temperatures above 400°C. Beside the solid solution hardening effect, the additions of alloying elements reduce the spheroidization and coarsening rate of the cementite, resulting in the fine particle distribution of cementite particles. Meanwhile, yield strength first increases up to 400°C and then continuously decreases with increasing tempering temperature. The occurrence of maximum peak of yield strength at 400°C would be related to further precipitation of the cementite at low tempering temperatures, and the subsequent spheroidization and coarsening process of the cementite at high tempering temperatures.
3. Charpy impact values were significantly influenced by tempering temperatures and alloying elements. It was also found that the minima of impact energy curves, related to tempered martensite embrittlement (TME), would be 400°C for all the tested steels. This would be because alloying elements do not have an influence on the decomposition of retained austenite and the formation of the cementite at boundaries.
4. The magnitude of strain-hardening exponent, n, decreases with tempering temperature up to 400°C and then continuously increases with increasing tempering temperature. This abrupt increase of n at the tempering

temperature of 300°C is related to the presence of retained austenite in induction-tempered steels. This austenite transforms to martensite during straining, and resultantly induces the high strain-hardening exponent in tempered steels.

References

1. K. Z. SHEPELYAKOVSKII and F. V. BEZMENOV, *Adv. Mater. Processes* **154** (1998) 225.
2. J. P. WISE, J. SPICE, S. G. DAVIDSON, W. E. HEITMANN and G. KRAUSS, *Scripta Mater.* **44** (2001) 299.
3. K. KAWASAKI, Y. SETO and T. YAMAZAKI, *Tetsu-to-Hagane* **71** (1985) 100.
4. K. KAWASAKI, T. CHIBA, N. TAKAOKA and T. YAMAZAKI, *ibid.* **73** (1987) 2290.
5. K. KAWASAKI, T. CHIBA and T. YAMAZAKI, *ibid.* **74** (1988) 334.
6. M. ASSEFPOUR-DEZFULY and A. BROWNRIGG, *Met. Trans.* **20A** (1989) 1951.
7. H. KAWAKAMI, Y. YAMADA, S. AAHIDA and K. SHIWAKU, in Proc. SAE Annual Cong., Detroit, MI, USA, February 1982, Society of Automotive Engineers, Paper 7, SAE Paper No. 820128, p. 1.
8. F. BORIK, V. A. BISS and Y. E. SMITH, in Proc. SAE Annual Cong., Detroit, MI, USA, February-March 1979, Society of Automotive Engineers, Paper 8, SAE Paper No. 790409, p. 1.
9. M. OHARA, K. UCHIBORI and K. CHISHIMA, *Mitsubishi Steel Manuf. Tech. Rev.* **15** (1981) 13.
10. C. H. SHIH, B. L. AVERBACH and M. COHEN, *Trans. ASM* **48** (1956) 86.
11. C. J. ALTSTETTER, M. COHEN and B. L. AVERBACH, *ibid.* **55** (1962) 287.
12. J. GORDINE and I. CODD, *J. Iron Steel Inst.* **207** (1969) 461.
13. N. SAITO, K. ABIKO and H. KIMURA, *Mater. Trans. JIM* **36** (1995) 601.
14. W. J. NAM, C. S. LEE and D. Y. BAN, *Mater. Sci. & Engin.* A **289** (2000) 8.
15. S. S. BABU, K. HONO and T. SAKURAI, *Met. & Mater. Trans.* A **25A** (1994) 499.
16. R. C. THOMSON and M. K. MILLER, *Appl. Surf. Sci.* **87/88** (1995) 185.
17. T. SAKUMA, N. WATANABE and T. NISHIZAWA, *Trans. JIM* **21** (1980) 159.
18. Y. J. PARK and I. M. BERNSTEIN, *Met. Trans.* A **10A** (1979) 1653.
19. T. TAKAHASHI, M. NAGUMO and Y. ASANO, *J. Jap. Inst. Metals* **42** (1978) 708.
20. G. R. SPEICH and W. C. LESLIE, *Met. Trans.* **3A** (1972) 1043.
21. K. A. PETERS, J. V. BEE, B. KOLK and G. G. GARRET, *Acta. Metall.* **37** (1989) 675.
22. W. J. NAM and H. C. CHOI, *Mater. Sci. & Tech.* **13** (1997) 568.
23. M. GENSAMER, *Trans. ASM* **36** (1946) 30.

Received 28 August 2002
and accepted 10 June 2003